Journal of Molecular Catalysis A: Chemical 308 (2009) 32–40

Contents lists available at ScienceDirect

Journal of Molecular Catalysis A: Chemical

journal homepage: www.elsevier.com/locate/molcata

Effect of morphology and crystallite size on solar photocatalytic activity of zinc oxide synthesized by solution free mechanochemical method

S.K. Pardeshi*, A.B. Patil

Department of Chemistry, University of Pune, Ganeshkhind, Pune 411007, India

ARTICLE INFO

Article history:
Received 19 January 2009
Received in revised form 14 March 2009
Accepted 16 March 2009
Available online 26 March 2009

Keywords:
Zinc oxide
Photocatalysis
Morphology
Sunlight
Resorcinol

ABSTRACT

Zinc oxide crystallites were synthesized by two steps, solution free mechanochemical method. In order to obtain zinc oxide of different morphology and crystallite size, calcination temperature was varied from 400 to 900 °C. These photocatalysts are then characterized by X-ray diffraction (XRD), Scanning Electron Micrograph (SEM), Energy dispersive X-ray spectra (EDXS), Fourier transform infrared spectra (FT-IR) and UV–Visible spectrophotometer. X-ray diffraction data suggest that the obtained ZnO crystallites are of wurtzite structure. The zinc oxide crystallite growth rate is found to be different in different calcination temperature range. Photocatalytic activity of ZnO was checked by means of oxidative photocatalytic degradation (PCD) of resorcinol a potent endocrine disrupter in water under irradiation of sunlight in a batch photoreactor. The PCD efficiency was found to be dependent on crystallite growth rate and morphology of zinc oxide. The zinc oxide calcined from 400 °C to 550 °C exhibit same crystallite growth rate and showed maximum photocatalytic degradation of resorcinol. The PCD efficiency of zinc oxide was found to decrease with increase in calcination temperature as the particle size was increased. In addition to effect of calcination temperature, the influence of various other parameters such as photocatalyst amount, initial concentration of resorcinol and pH was also examined for maximum PCD of resorcinol. Neutral and basic pH is found to be favorable for chemical oxygen demand (COD) removal of resorcinol.

1. Introduction

The photocatalytic degradation of organic pollutants in water and air, using semiconductors such as TiO_2 and ZnO have attracted more attention due to its incomparable ability in the environmental detoxification [1–5]. The advantage of photocatalytic process is that it works at ambient conditions of temperature and pressure without forming any kind of sludge, which otherwise creates another pollution problem.

Among the semiconductors whose photocatalytic properties have been studied, TiO_2 is the most commonly used, because it is stable, harmless, and inexpensive [6]. However, TiO_2 is only excited by UV light [7,8]. Use of ultra violet light is not much feasible and economical. Recently zinc oxide has been received more attention from researchers. Zinc oxide is well known semiconductor under solar irradiation, and its photocatalytic mechanism has been proved to be similar to that of TiO_2 [9]. Zinc oxide has been reported to be more efficient than TiO_2 in some of the process such as the advanced oxidation of pulp mill bleaching waste water [10]. The biggest advantage of ZnO is that it absorbs over a larger fraction of the solar spectrum than TiO_2 [11]. For this reason, ZnO is the most suitable photocatalyst for photocatalytic oxidation of organic compounds in the presence of sunlight. In the countries where ample amount of sunlight is available, photocatalysis involving sunlight will be economical and preferable as solar light contains ca. 43% visible and ca. 4% Ultra Violet light, which is free and inexhaustible [12]. When Zinc oxide particles are illuminated with solar light or near UV radiation, the initial step in the ZnO-mediated photocatalyzed degradation is proposed to involve the generation of an (e^-/h^+) pair leading to the formation of hydroxyl radical ($^\bullet OH$), superoxide radical anions ($O_2{}^{-\bullet}$), and hydroperoxyl radical ($^\bullet OOH$). The hydroxyl radicals are known to be powerful and non-selective oxidizing agents ($E^0 = +3.06$ V), which are responsible for partial or complete mineralization of several organic chemicals [13]. Moreover, the high oxidative potential of the holes ($h_{vb}{}^+$) in the photocatalyst also permits the direct oxidation of organic substance to reactive intermediates. Very reactive hydroxyl radicals also be formed either by the decomposition of water or by the reaction of the hole with OH^-. The degradation efficiency depends on the oxygen concentration, determining the efficiency with which conduction band electrons ($e^-{}_{cb}$) are scavenged or the recombination of (e^-/h^+) is prevented. The electron in the conduction band can be picked up by the adsorbed substrate molecules, leading to the formation of radical anion and the degradation of the organic substance [14]. In order to prevent recombination of e^-/h^+ and hence to improve visible light photocatalytic activity of ZnO lot of efforts

* Corresponding author. Tel.: +91 020 25601394x514; fax: +91 020 25691728.
E-mail address: skpar@chem.unipune.ernet.in (S.K. Pardeshi).

1381-1169/$ – see front matter © 2009 Elsevier B.V. All rights reserved.
doi:10.1016/j.molcata.2009.03.023

have been made. Rongliang et al. [15] studied visible light photocatalytic activity of polymer modified ZnO. Combination effect of ZnO and activated carbon for solar assisted photocatalytic degradation was investigated by Sobana and Swaminathan [16]. Parida and Parija [17] studied the effect of preparation method on photocatalytic activity of ZnO towards the photooxidation of 0.01 g/l (10 ppm) phenol under sunlight in closed Pyrex flasks at room temperature. They have reported 88% degradation at pH 5. The photocatalytic activity also depends upon the crystallinity, surface area and particle morphology [18]. Fang et al. [19] and Seow et al. [20] synthesized semiconductor oxides of different morphology. It has been proved that crystallinity; surface area and particle morphology of material are important factors determining photocatalytic activity. Recently, photocatalytic activity of hierarchically sponge-like macro-/mesoporous TiO_2 [21,22] hollow microspheres of WO_3 [23] polycrystalline flakes with a hierarchical architecture of Bi_2WO_6 [24] hollow spheres with porous crystalline shells of ZnO [25] were reported. The morphology and crystallinity depends upon the method of preparation and calcination temperature.

In present article, we are reporting the solar photocatalytic activity of zinc oxide synthesized by solution free mechanochemical method and effect of calcination temperature on photocatalytic degradation of resorcinol, a model endocrine disrupter [26]. In addition to effect of morphology and crystallite growth rate, other parameters such as amount of photocatalyst, concentration of substrate, pH, etc. on photocatalytic degradation (PCD) efficiency is also studied.

2. Experimental

2.1. Materials

In present study, zinc acetate (assay ≥ 98%) oxalic acid (assay 99.5%), resorcinol (assay 99%) and other required chemicals are of analytical grade, obtained from Merck Limited, Mumbai, India and were used without further purification. The appropriate concentration of resorcinol solutions was prepared by using double distilled water. The pH of the solutions were adjusted to desired values from 4 to 10 by using dilute solution of H_2SO_4 (0.01N) and NaOH (0.01N).

2.2. Synthesis of photocatalyst

Zinc oxide crystallite was prepared by solution free mechanochemical method [27]. In a typical synthesis, 0.1 mol of zinc acetate and 0.12 mol of oxalic acid were mixed by grinding in an agate mortar for 30 min at room temperature, forming the zinc oxalate dihydrate ($ZnC_2O_4{\cdot}2H_2O$). The zinc oxalate thus obtained was tested by Thermo gravimetric analysis and FT-IR. Zinc oxide crystallite was then prepared by thermal decomposition of the obtained zinc oxalate. In order to obtain zinc oxide of different morphology and crystallite size, calcination temperature was varied from 400 °C to 900 °C. The X-ray diffraction (XRD) pattern of the final ZnO crystallite was obtained with Cu Kα radiation (λ = 1.5406 Å) on X-ray Diffractometer (D-8 Advance Brkur AXS) and the mean grain size (D) of the particles was determined from the XRD line-broadening measurement from the Deby-Scherer equation [28] as follows:

$$D = \frac{0.89\lambda}{(\beta \cos\theta)} \quad (1)$$

where λ is the wavelength (Cu Kα), β is the full width at the half-maximum of the ZnO (1 0 1) line and θ is the diffraction angle. The peak positions and relative intensities were characterized by comparison with the Joint Committee for Powder Diffraction Standards (JCPDS) card no 36-1451 for examining the phase structure and purity. The conversion of zinc oxalate to zinc oxide was studied by FT-IR (Shimadzu FTIR-8400 spectrometer equipped with KBr beam splitter). Morphological characterization of the product was performed using SEM. Energy dispersive X-ray spectra (EDXS) measured by a SEM attachment were used for the elemental characterization of the photocatalyst. Mechanism of ZnO crystallite growth was investigated as per Scott equation [29].

2.3. Photocatalytic degradation experiments

The photocatalytic degradation efficiency of zinc oxide of different morphology and crystallite size was investigated by means of solar PCD of resorcinol. All PCD experiments were carried out in duplicate and at ambient temperature. It should also be noted that no external supply of oxygen was employed. Pure resorcinol (Merck, 99%) was dissolved in double distilled water to obtain desired concentration solutions. In all PCD experiments, 100 ml resorcinol solution of appropriate concentration was taken in batch photocatalytic reactor vessel. A known quantity of ZnO calcined at a certain temperature was added and mixture was agitated in an ultrasonic bath for 5 min to obtain uniform suspension. Initial pH of suspension was recorded. Whole setup was then placed in sunlight with constant stirring for specific period of time. When PCD reaction was stopped after the desired time of sunlight irradiation, whole suspension was centrifuged at a speed of 5000 rpm for 5 min (Remi, India) and then filtered through a 0.45 μm Polytetrafluro ethylene (PTFE) filters. The liquid portion was used for absorbance and COD measurement.

2.4. Equipments and light source

Photocatalytic reactions were carried out in batch photoreactor which configures with cylindrical glass vessel (200 ml capacity), condensation tube, quartz cool trap and magnetic stirrer. The extent of PCD at an interval of one hour sunlight irradiation was primarily checked by means of decrease in absorbance on UV–Visible Spectrophotometer (UV-1601, Shimadzu). Complete mineralization of resorcinol was ensured by chemical oxygen demand (COD) reduction method. The COD determination tests were performed according to standard dichromate method using COD digester [30]. The PCD efficiency was calculated from the following expression (2).

$$\eta = \frac{COD_i - COD_t}{COD_i} \times 100 \quad (2)$$

where η—Photocatalytic degradation efficiency, COD_i—Initial chemical oxygen demand, COD_t—Chemical oxygen demand at time t. The pH of suspension was measured with pH meter (EUTECH-pH510). All PCD experiments were performed under irradiation of sunlight between 9:00 a.m. and 5:00 p.m. during the months of December to March. The intensity of sunlight was periodically checked by ferrioxalate actinometry [31]. The average photon flux calculated for entire duration of irradiation of sunlight was found to be 1.7×10^{-7} Einstein s^{-1} cm^{-2}.

The reusability of the photocatalyst was evaluated by reclaiming the photocatalyst after PCD reaction in the batch mode, washing, drying in electric oven at 110 °C and using it for resorcinol degradation under similar experimental conditions.

2.5. Dark adsorption studies

The adsorption of resorcinol in dark on the surface of ZnO was investigated. In typical experiments, 100 ml of resorcinol solution (100 ppm) was taken in batch photoreactor vessel. Natural pH of this solution was 6.8. To this solution 250 mg ZnO calcined at 400 °C (MCM400) was added and resulting suspension was stirred in dark for 7 h. Then the suspension was centrifuged and filtered. Filtrate

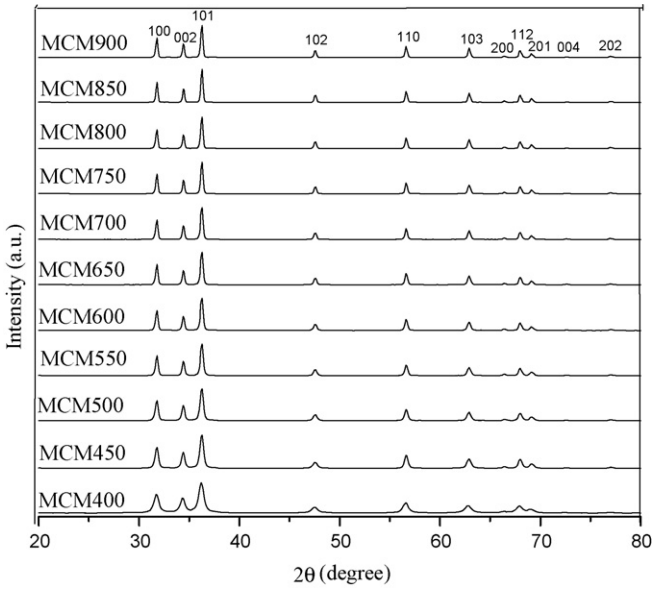

Fig. 1. XRD pattern of zinc oxide samples calcined from 400 °C (MCM400) to 900 °C (MCM900).

was used for UV–Visible absorbance measurement and COD determination.

3. Result and discussion

3.1. Characterization of photocatalysts

3.1.1. XRD analysis

Fig. 1 shows XRD pattern of the ZnO crystallite samples calcined at 400–900 °C. The diffraction peaks can be indexed as hexagonal wurtzite structure of ZnO (a = 3.249 Å, c = 5.206 Å) and diffraction data were in good agreement with the JCPDS card for ZnO (JCPDS 36-1451). As calcination temperature increases the XRD pattern of ZnO phase becomes higher and sharper (Fig. 1). The crystallite size of ZnO was estimated by Scherer's formula (Eq. (1)). This was found to increase from about 31.8 nm at 400°C to 75.2 nm at 900 °C (Table 1).

3.1.2. TG-DTG analysis

The TGA-DTG curves of the powder mixture after grinding for 30 min are shown in Fig. 2. There are two major weight loss processes from 30 °C to 390 °C in TG. The weight losses centered at 60 °C and 120 °C corresponding to a 3.3% and 23% respectively are due to both the release of the remaining acetic acid byproduct and the conversion of zinc oxalate dihydrate to anhydrous zinc oxalate, i.e. loss of two water of crystallization molecules. The acetic acid molecules easily volatize into air, we can smell acidic gas generated during the grinding. However, the acetic acid has a boiling point of 118 °C, so the remaining acetic acid can only be totally removed at a temperature higher than its boiling point. Therefore, it is reasonable that the total 26.3% weight loss at temperatures below 300 °C is larger than the theoretical crystal water content of 19.03% in pure $ZnC_2O_4{\cdot}2H_2O$. The weight loss of 35.8% occurs at 340–390 °C is attributed to the conversion of anhydrous zinc oxalate to zinc oxide. The DTG curve shows two major peaks corresponding to the weight losses in TGA curve. The result is summarized in Table 2. From TG-DTG analysis it is confirmed that zinc oxalate is completely converted in to zinc

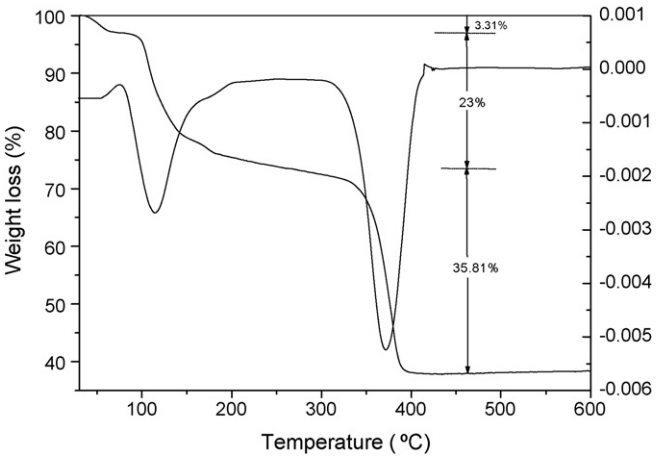

Fig. 2. TG-DTG curves for conversion of zinc oxalate to zinc oxide.

Table 2
TG-DTG data for conversion of zinc oxalate to zinc oxide.

Step	Temperature (°C)	Weight loss (%)	
		Theoretical	Observed
I and II	25–120	19	26.3
III	120–390	36	35.8

Table 1
Effect of calcination temperature on PCD efficiency of ZnO.

Photocatalyst	Calcination temperature (°C)	Band gap (eV)	D (nm)	COD_t (ppm)	η (%)
MCM400[a]	400	3.345	31.8	0	100
MCM450	450		38.9	0	100
MCM500	500	3.319	44.1	0	100
MCM550	550		51.9	3.45	98
MCM600	600	3.310	54	36.8	79
MCM650	650		56.67	69	60
MCM700	700	3.292	60.15	113.9	34
MCM750	750		62	118.7	31.2
MCM800	800	3.275	64	121.6	29.5
MCM850	850		70.9	142	17.6
MCM900	900	3.258	75.19	156.4	9.3

[Resorcinol] = 100 ppm, Initial COD (COD_i) = 173 ppm, Initial pH of suspension = Natural (6.8), Amount of photocatalyst = 250 mg/100 ml, Sunlight irradiation time = 7 h.
Intensity of sunlight = 1.7×10^{-7} Einstein s^{-1} cm^{-2}.
[a] Zinc oxide synthesized by Mechanochemical method and calcined at 400 °C.

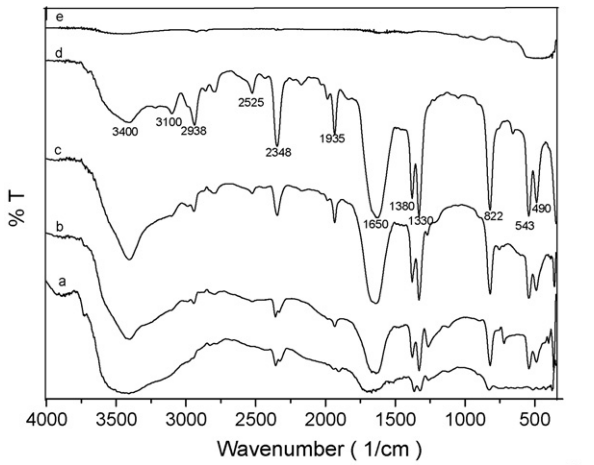

Fig. 3. FT-IR spectra for conversion of zinc oxalate to zinc oxide.

oxide at 400 °C. It is further supported by XRD and FT-IR analysis data.

3.1.3. FT-IR analysis

When zinc acetate and oxalic acid were mixed by grinding in an agate mortar for 30 min at room temperature, zinc oxalate dihydrate was formed. Zinc oxide was further obtained by thermal decomposition of zinc oxalate. In order to observe the progress of conversion of zinc oxalate to zinc oxide by means of FT-IR spectra, zinc oxalate was stepwise thermally treated at 100 °C, 200 °C, 300 °C and 400 °C. Fig. 3 shows the changes in FT-IR spectra during the thermal decomposition of zinc oxalate in to zinc oxide. The intense broad band at 3400 cm^{-1} represents (Fig. 3 a–d) the stretching vibration of H—O in crystal water. Another broad band at 1650 cm^{-1} is superposed by the stretching vibration of C=O and bending vibration of H—O—H. The 3400 cm^{-1} and 1650 cm^{-1} bands were found to be sharper as the temperature was increased. When zinc oxalate precursor was calcined at 300 °C, the1650 cm^{-1} band was found to be more intense at the same time the 3400 cm^{-1} band was found to be less broader as compare to the same bands of zinc oxalate before heat treatment and calcined at 100 °C and 200 °C. This shows that up to 300 °C most of water of crystallization of zinc oxalate gets removed to form anhydrous zinc oxalate. This fact was also supported by TG-DTG analysis (Fig. 2). The bands 1380 cm^{-1} and 1330 cm^{-1} are due to the stretching vibration of C—O and that at 490 cm^{-1} is because of typical Zn—O bonding. When calcination temperature was increased to 400 °C except 490 cm^{-1} no other bands were detected (Fig. 3e). Thus, the formation of pure ZnO crystal at 400 °C is approved by FT-IR. This is further confirmed by XRD and EDXS.

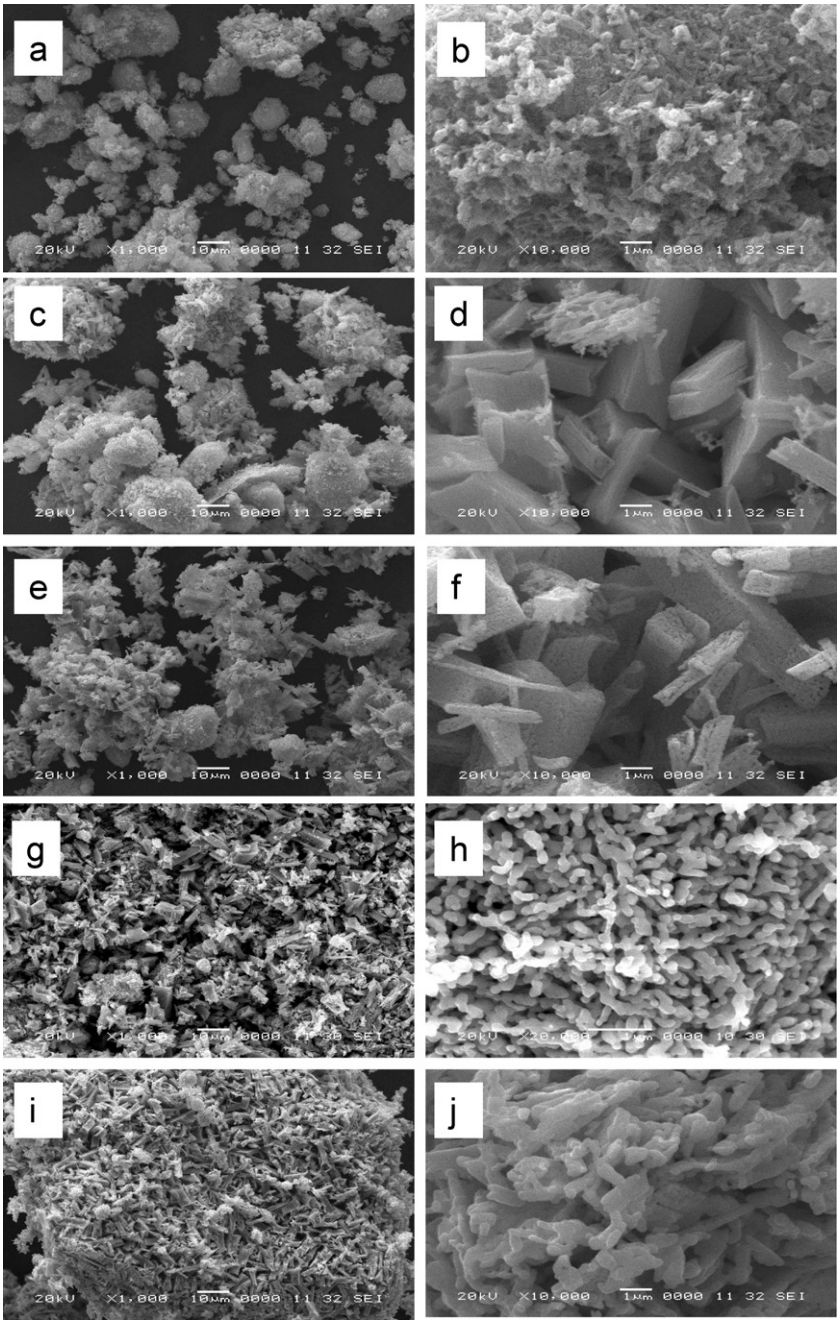

Fig. 4. SEM images of MCM400 (a, b), MCM500 (c, d), MCM600 (e, f), MCM700 (g, h), MCM800 (i, j).

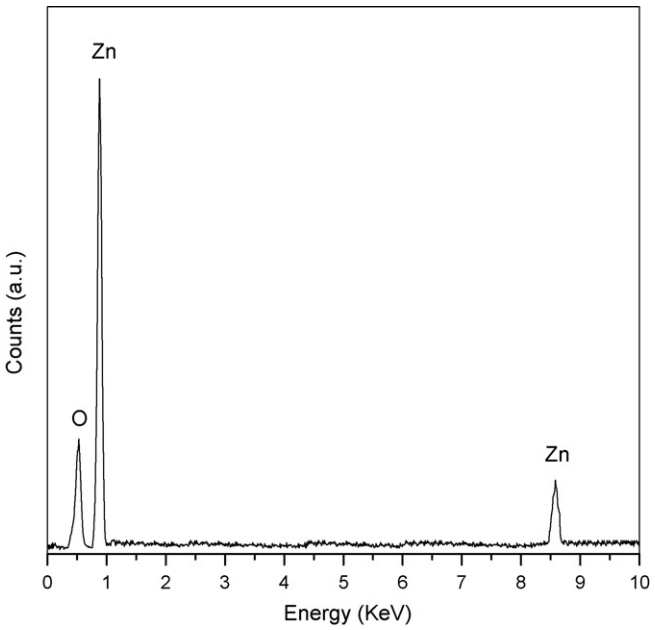

Fig. 5. Energy dispersive X-ray spectra of zinc oxide sample calcined at 400 °C.

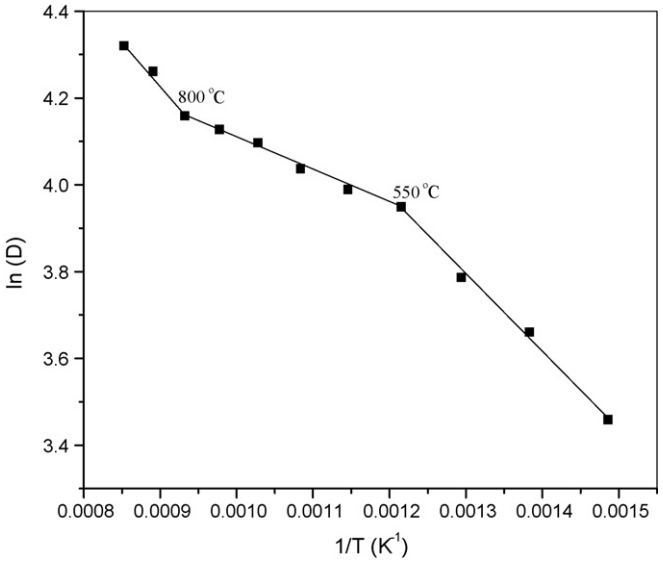

Fig. 6. Plot of ln(D) versus 1/T of ZnO samples calcined from 400 °C to 900 °C.

3.1.4. SEM-EDXS analysis

The surface morphology and crystallite structure of calcined powder were analyzed using Scanning Electron Microscope (SEM) studies. Morphology of ZnO was found to be greatly affected by calcination temperature (Fig. 4a–j). The SEM images confirm that ZnO exists in single homogeneous phase with a porous sponge-like structure. Energy dispersive X-ray spectrum (EDXS) of MCM400 is shown in Fig. 5. It shows peaks corresponding to Zn and O, no trace amount of other impurities could be seen in the detection limit of the EDXS.

3.1.5. Mechanism of ZnO crystallite growth

The graph of ln(D) against 1/T shows straight lines according to the Scott equation (Eq. (3)) on the assumption that ZnO crystallite growth is homogeneous [26], which approximately describes the crystallite growth during annealing.

$$D = C \exp\left(\frac{-E}{RT}\right) \quad (3)$$

where D is the XRD average crystal size, C is a constant, E is activation energy for crystallite growth, R is the gas constant and T is absolute temperature.

The plot of ln(D) against 1/T is shown in Fig. 6. There are three straight lines of different slopes from 400 °C to 900 °C. The slope of first line changes at 550 °C and that of second line changes at 800 °C. The activation energies E_1, E_2 and E_3 corresponding to crystal growth during 400–550 °C, 550–800 °C and 800–900 °C are obtained by Scott equation and found to be 1.88 kJ/mol, 2.48 kJ/mol and 2.36 kJ/mol respectively. This shows that the ZnO crystallite growth rate is different in different temperature range due to the interfacial reaction during calcination. It is very interesting to note that zinc oxide obtained at three different crystallite growth rate showed different photocatalytic activity because of different morphology and crystallite size. The detail explanation of this is given in Section 3.2.1.

3.1.6. UV–Visible analysis

Typical UV–Visible spectra of zinc oxide obtained at various calcination temperatures are shown in Fig. 7. It is observed that with increase in calcination temperature absorption wavelength of zinc oxide shifts towards longer wavelength. This results in the narrowing of band gap from 3.345 eV for MCM400 to 3.275 eV for MCM800 as shown in Fig. 8. The narrowing of band gap may be beneficial for solar light mediated photocatalysis as it helps to absorb light of longer wavelength but at the same time it also makes easy recombination between valance band holes and conduction band electrons. The exact correlation for the same is explained in Section 3.2.1.

3.2. Photocatalytic activity study

The photocatalytic nature of ZnO, effect of calcination temperature, amount of photocatalyst, substrate concentration, irradiation time and pH on the efficiency of resorcinol degradation was examined and the results are discussed in the following subsections.

3.2.1. Effect of calcination temperature

Photocatalytic efficiency of ZnO depends upon morphology and particle size [17]. Morphology and crystallite size of ZnO have been changed by varying calcination temperature from 400 °C to 900 °C (Fig. 8). The PCD efficiency of ZnO calcined from 400 °C to 900 °C was then investigated by means of solar photocatalytic degradation of

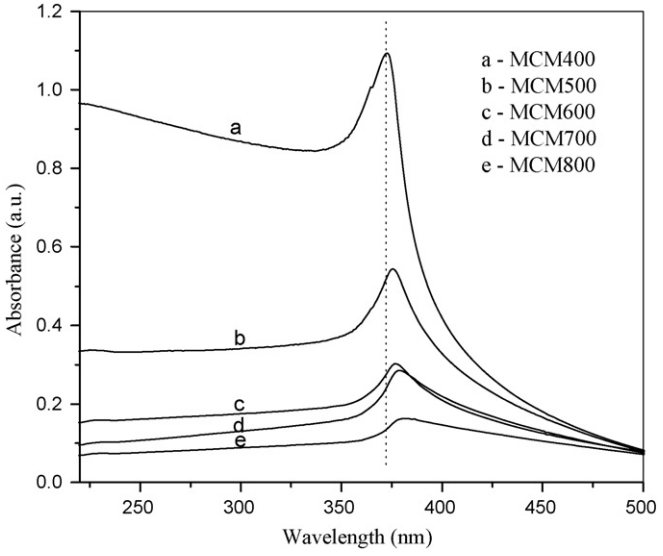

Fig. 7. UV–Visible spectra of zinc oxide samples calcined from 400 °C to 800 °C.

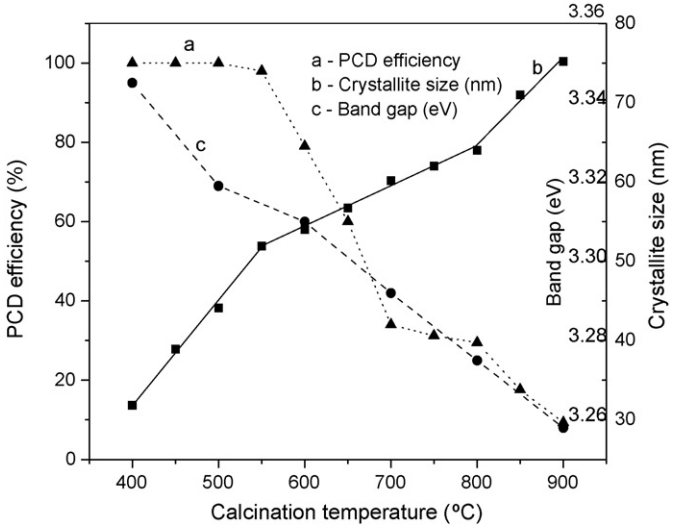

Fig. 8. Effect of calcination temperature on photocatalytic degradation efficiency.

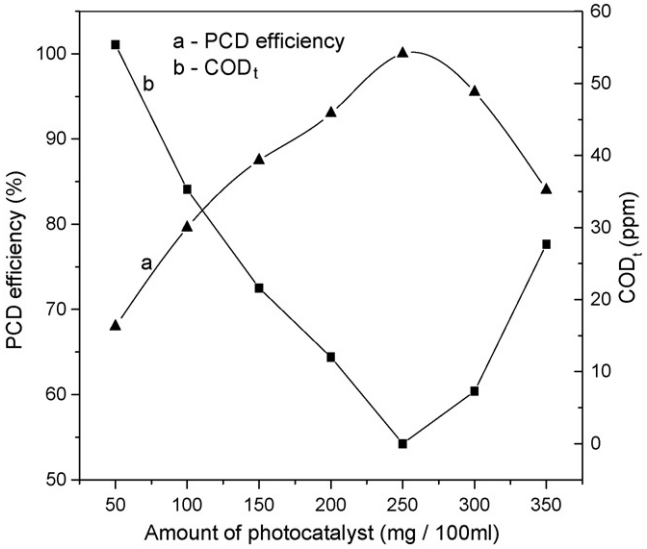

Fig. 9. Effect of amount of photocatalyst on photocatalytic degradation efficiency.

resorcinol. Zinc oxide calcined from 400 °C to 550 °C showed about 100% PCD efficiency even though particle size of ZnO increases from 31.8 nm to 51.9 nm. This may be due to the fact that crystallite growth rate for ZnO calcined up to 550 °C was uniform (1.88 kJ/mol), which gives ZnO of same morphology. After 550 °C the PCD efficiency of ZnO was found to decrease with increase in calcination temperature. This may be due to fact that with increase in calcination temperature, crystallite size of ZnO increases, therefore surface area decreases which leads to decrease in number of active sites of photocatalyst for adsorption of substrate molecules. It is important to note that the crystallite growth rate in temperature range 550–800 °C was found to be different than that of 400–550 °C, with higher activation energy (2.48 kJ/mol). An analogous observation was reported by Ao et al. [32] stating that the different ZnO crystallite growth rate in different temperature range is due to the different interfacial reaction during calcinations. Thus different morphology of ZnO is affecting its PCD efficiency. When calcination temperature was increased beyond 800 °C, activation energy of zinc oxide crystallite growth was slightly decreased (2.36 kJ/mol) but at the same time particle size were greatly increased which showed negative effect on PCD efficiency (Fig. 8). Zinc oxide calcined at 400 °C (MCM400) showed 100% photocatalytic degradation of 100 ppm resorcinol within 7 h. This was the lowest possible calcination temperature at which photocatalytically active ZnO forms. Therefore MCM400 was selected for the study of effect of other parameters such as effect of amount of photocatalyst, concentration of substrate, pH and irradiation time.

3.2.2. *Effect of the photocatalyst amount*

Blank experiments were carried out without photocatalyst to examine the extent of resorcinol 'photolyzed' in the absence of photocatalyst. No detectable PCD of resorcinol was evidenced in aqueous solution in the absence of ZnO. When aqueous solution of resorcinol containing ZnO (MCM400) was irradiated with sunlight, PCD of resorcinol was observed. The optimum amount of photocatalyst required for maximum PCD of resorcinol was examined in slurry method by varying photocatalyst amount from 50 to 350 mg in 100 ml resorcinol solution (100 ppm) at its natural pH. The PCD of resorcinol was found to increase with increase in amount of ZnO up to 250 mg, further increase in photocatalyst amount showed negative effect. The results obtained are illustrated in Fig. 9. At lower photocatalyst loading level than the optimum amount, photonic absorption controls the efficiency of PCD due to limited surface area of photocatalyst therefore efficiency of PCD increased linearly with increase in photocatalyst loading up to 250 mg. The increase in the amount of photocatalyst increased the number of active sites on the photocatalyst surface, which in turn increased the number of hydroxyl, and superoxide radicals. When the quantity of ZnO was increased above the limiting value, the degradation rate was decreased. This may be due to an increase in the turbidity of the suspension, which affects the penetration of sunlight as a result of increased screening effect and scattering of light [33]. Another reason may be that after the optimum amount of ZnO, photocatalyst surface probably becomes unavailable for photoabsorption because of agglomeration and sedimentation of ZnO particles [34]. Thus 250 mg of ZnO was selected as optimum amount for the study of other parameters.

3.2.3. *Effect of the initial concentration of resorcinol*

The PCD of resorcinol at different initial concentrations in the range 50–350 ppm was investigated as a function of sunlight irradiation time at the natural pH of suspension (without adjustment). The results are illustrated in Fig. 10. Resorcinol solutions up to 100 ppm were completely mineralized by using 250 mg/100 ml of

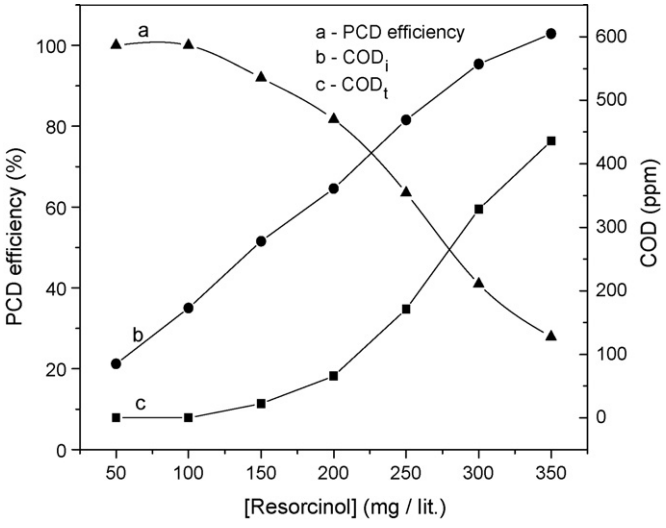

Fig. 10. Effect of concentration of resorcinol on photocatalytic degradation efficiency.

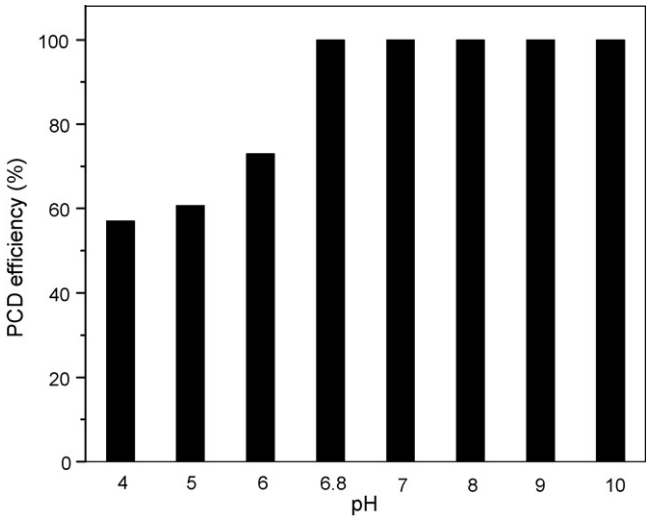

Fig. 11. Effect of initial pH of suspension on photocatalytic degradation efficiency.

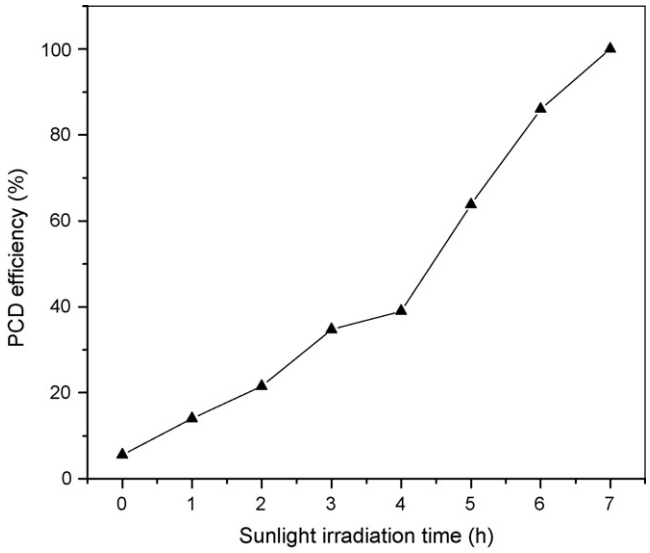

Fig. 12. Effect of sunlight irradiation time on photocatalytic degradation efficiency.

zinc oxide. However after 100 ppm, PCD was found to be inversely affected by concentration of resorcinol.

This may be due to the fact that as the initial concentration of resorcinol increases, more and more resorcinol molecules are adsorbed on the surface of ZnO, but the number of $^{\bullet}OH$ and $^{\bullet}O_2^-$ radicals formed (Scheme 1a–e) on the surface of ZnO and the irradiation time are constant. Therefore relative number of $^{\bullet}OH$ and $^{\bullet}O_2^-$ radicals available for attacking the substrate becomes less in comparison to resorcinol molecules. Hence photodegradation decreases. Also, as the concentration of resorcinol increases, the photons get interrupted before they can reach the photocatalyst surface hence absorption of photons by the photocatalyst decreases and consequently the PCD was reduced. Hence under given set of conditions, the maximum concentration of resorcinol that could be degraded by 250 mg of ZnO is found to be 100 ppm. Thus 100 ppm resorcinol was selected as optimum concentration for the study of other parameters. Thus 100 ppm resorcinol was selected as optimum concentration for the study of other parameters.

3.2.4. Effect of initial pH

Most of the semiconductor oxides are amphoteric in nature therefore pH of suspension is an important parameter governing the PCD reaction taking place on semiconductor particle surface. It influences surface charge properties of photocatalyst [35]. The effect of initial pH of suspension on PCD efficiency was studied from 4 to 10 with 100 ppm resorcinol solution and 250 mg/100 ml ZnO loading. The pH of the suspension was adjusted before irradiation of sunlight and it was not controlled during the course of reaction. All other parameters were kept constant. In acidic medium less PCD of resorcinol was observed. This may be due to slight dissolution of ZnO at low pH [11]. The extent of PCD of resorcinol was found to increase with increase in initial pH of suspension exhibiting maximum PCD in the alkaline pH (Fig. 11). In alkaline medium, excess of hydroxyl anions facilitate photo generation of $^{\bullet}OH$ radicals (Scheme 1c) which is accepted as primary oxidizing species responsible for PCD [36,37]. This increases PCD efficiency. Natural pH of 100 ppm resorcinol is 6.8. This solution also shows 100% degradation therefore other parameters were studied at natural pH of 100 ppm resorcinol.

3.2.5. Effect of irradiation time

The PCD of 100 ppm resorcinol in sunlight was found to increase with increase in irradiation time and within seven hours there was 100% degradation (Fig. 12). When 100 ppm resorcinol solution along with ZnO is magnetically stirred for seven hours in the absence of light (dark), negligible (5.5%) photodegradation was observed. For reference it is considered as zero hour irradiation. It is observed that with increase in irradiation time, the absorbance of resorcinol at 274 nm (λ_{max}) decreases and after 7 h irradiation of sunlight it falls to zero (Fig. 13). Thus zinc oxide synthesized by solution free mechanochemical method is an effective photocatalyst in sunlight.

4. Photodegradation mechanism

When milky white suspension of aqueous solution of resorcinol and ZnO was irradiated with sunlight, the white suspension was gradually changed to brown. The intensity of brown color was found to increase up to 4 h irradiation and then it was decreased. For the resorcinol solution up to 100 ppm, after 7 h irradiation white suspension was reappeared. The brown color of the photoreaction mixture was probably due to formation of various reaction intermediates viz. 3-hydroxyl phenoxy radical, 1,2,4 tri hydroxyl benzene, 1,2,3 trihydroxyl benzene, etc. The probable PCD mechanism is

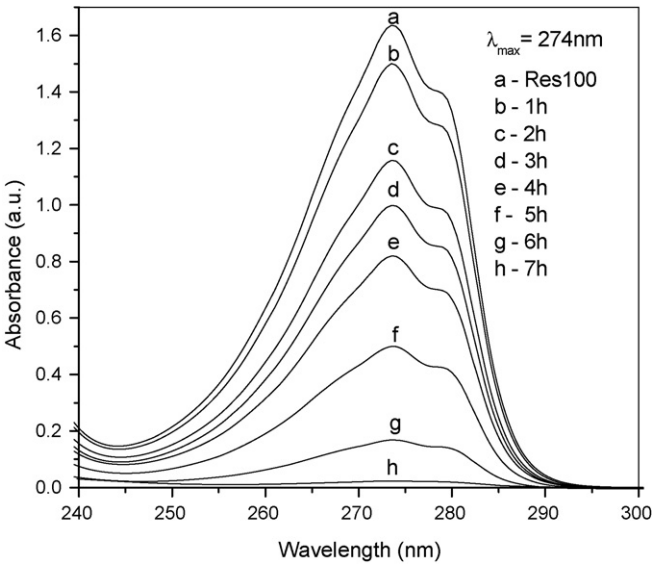

Fig. 13. UV–Visible spectra showing photocatalytic degradation of resorcinol.

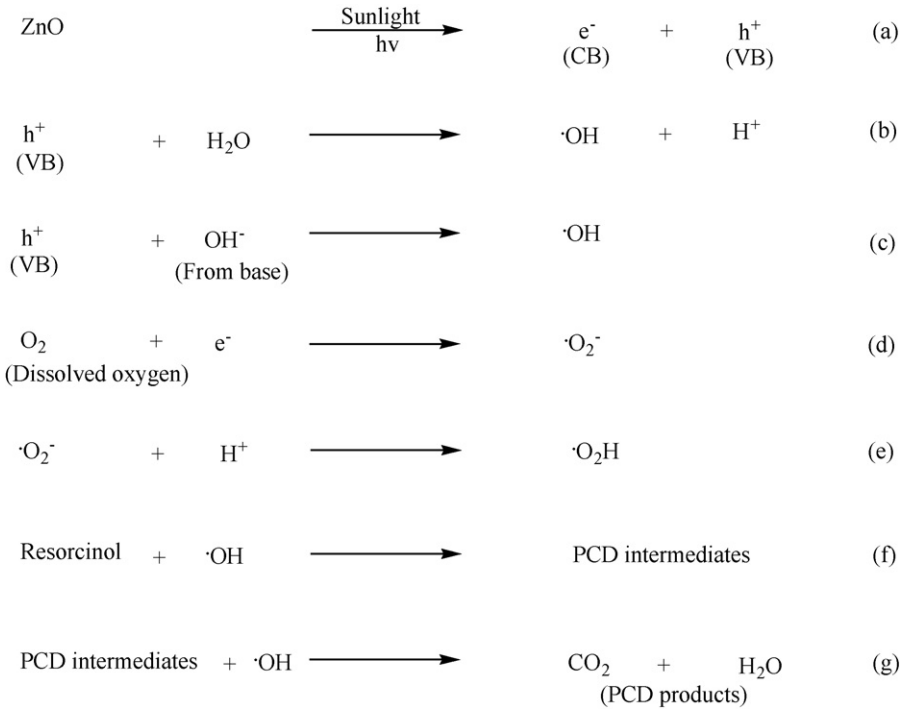

Scheme 1. Photocatalytic degradation of resorcinol over ZnO under irradiation of sunlight.

shown in Scheme 1a–g. The excitation of ZnO by solar energy leads to the formation of an electron–hole pair (Scheme 1a). The hole combines with water or base to form •OH radicals (Scheme 1b, c) while electron converts dissolved oxygen to super oxide radical ($^{\bullet}O_2^-$), a strong oxidizing species and hydroperoxyl radical ($^{\bullet}OH_2$) (Scheme 1d, e). The •OH radicals initially converts resorcinol in to PCD intermediates and then in to PCD products, i.e. CO_2 and H_2O (Scheme 1f, g). The PCD mechanism and identification of various PCD intermediates have been already reported [38].

5. Reuse of photocatalyst

At the time of study of effect of various parameters, for every photo catalytic degradation experiment fresh ZnO was used. Reuse of ZnO was separately studied, by keeping all other parameters constant. During this study, after sunlight irradiation for seven hours, photoreaction mixture was centrifuged and filtered. Filtrate was used for COD determination and ZnO residue was washed several times with double distilled water in ultrasonic bath followed by filtration and drying at 110 °C in an electric oven. Recovered ZnO (MCM400) was then reused for new photodegradation batch, without any further treatment such as heating in any kind of furnace. All photo catalytic degradation experiments are carried out in duplicate, under sunlight. Activity of recycled MCM400 ZnO was found to retain even after fifth photodegradation experiment. The reusability of ZnO is due to its stability in neutral solution and negligible photocorrosion [39].

6. Conclusions

In present study ZnO was synthesized by solution free mechanochemical method and was found to be a better photocatalyst in sunlight for degradation of resorcinol.

1. PCD efficiency of ZnO was found to be greatly affected by morphology and crystallite size.
2. Low calcination temperature, smaller crystallite size of zinc oxide and basic pH of suspension were favorable for photocatalytic degradation.
3. Resorcinol solutions of 100 ppm concentration were completely mineralized by photocatalytic degradation on the surface of ZnO calcined at 400–550 °C, under irradiation of sunlight.
4. ZnO can be reused for five times as it undergoes photocorrosion only to the negligible extent.
5. Higher concentration solution of phenols may be completely mineralized by modified ZnO, which is our current interest of research.

References

[1] B. Swarnalata, Y. Anjaneyulu, J. Mol. Catal. A: Chem. 223 (2004) 161–165.
[2] C.C. Chen, J. Mol. Catal. A: Chem. 264 (2007) 82–92.
[3] A. Akyol, M. Bayramoglu, J. Hazard. Mater. B 124 (2005) 241–246.
[4] M.J. Height, S.E. Pratsinis, O. Mekasuwandumrong, P. Praserthdam, Appl. Catal. B: Environ. 63 (2006) 305–312.
[5] S.K. Pardeshi, A.B. Patil, Sol. Energy 82 (2008) 700–705.
[6] S.B. Dhananjay, G.P. Vishwas, B. Anthony, J. Chem. Technol. Biotechnol. 77 (2001) 102–116.
[7] K. Honda, A. Fujishima, Nature 238 (1972) 37.
[8] I. Sopyan, M. Watanabe, S. Murasawa, K. Hashimoto, A. Fujishima, J. Photochem. Photobiol. 98 (1996) 79.
[9] B. Dindar, S. Icli, J. Photochem. Photobiol. A: Chem. 140 (2001) 263–268.
[10] M.C. Yeber, J. Roderiguez, J. Freer, J. Baeza, N. Duran, H.D. Mansilla, Chemosphere 39 (1999) 10–16.
[11] M.A. Behnajady, N. Modirshahla, R. Hamzavi, J. Hazard. Mater. B 133 (2006) 226–232.
[12] S. Sakthivel, H. Kish, Chem. Phys. Chem. 4 (2003) 487–490.
[13] A. Mills, S. LeHunte, J. Photochem. Photobiol. 108 (1) (1997) 1–35.
[14] H. Lachheb, E. Puazenat, A. Houas, M. Ksibi, E. Elaloui, C. Guillard, J.M. Herrman, Appl. Catal. B: Environ. 39 (2002) 75.
[15] R. Qiu, D. Zhang, Y. Mo, L. Song, E. Brewer, X. Huang, Y. Xiong, J. Hazard. Mater. 156 (2008) 80–85.
[16] N. Sobana, M. Swaminathan, Sol. Energy Mater. Sol. Cells 91 (2007) 727–734.
[17] K.M. Parida, S. Parija, Sol. Energy 80 (2006) 1048–1054.
[18] D. Li, H. Hadeda, Chemosphere 51 (2003) 129.
[19] F. Lei, B. Yan, J. Phys. Chem. C 113 (2009) 1074–1082.
[20] Z.L.S. Seow, A.S.W. Wong, V. Thavasi, R. Jose, S. Ramakrishna, G.W. Ho, Nanotechnology 20 (2009) 045604.
[21] J. Yu, L. Zhang, B. Cheng, Y. Su, J. Phys. Chem. C 111 (2007) 10582–10589.
[22] J.G. Yu, Y.R. Su, B. Cheng, Adv. Funct. Mater. 17 (2007) 1984–1990.

[23] J. Yu, H. Yu, H. Guo, M. Li, S. Mann, Small 4 (2008) 87–91.
[24] F. Amano, K. Nogami, B. Ohtani, J. Phys. Chem. C 113 (2009) 1536–1542.
[25] J. Yu, X. Yu, Environ. Sci. Technol. 42 (2008) 4902–4907.
[26] J.J. Amaral, Mendes, Food Chem. Technol. 40 (2002) 781–788.
[27] L. Shen, N. Bao, K. Yanagisawa, K. Domen, A. Gupta, C.A. Grimes, Nanotechnology 17 (2006) 5117–5123.
[28] H.P. Klug, L.E. Alexander, X-ray Diffraction Procedures for Polycrystalline and Amorphous Materials, 1st ed., Wiley, New York, 1954 (Chapter 9).
[29] M.G. Scott, Amorphous Metallic Alloys, Butter-Worths Co. Ltd., London, 1983.
[30] J.T. Bellaire, G.A. Parr-Smith, Standard Methods for the Examination of Water and Wastewater, 17th ed., Am Public Health Association, Washington, DC, 1985.
[31] C.G. Hatchard, C.A. Parker, Proc. R. Soc. London A235 (1956) 518.
[32] W. Ao, J. Li, H. Yang, X. Zeng, X. Ma, Powder Technol. 168 (2006) 148–151.
[33] S. Anandan, A. Vinu, N. Venkatachalam, B. Arabindoo, V. Murugesan, J. Mol. Catal. A: Chem. 256 (2006) 312–320.
[34] C.M. So, M.Y. Cheng, J.C. Yu, P.K. Wong, Chemosphere 46 (2002) 905–912.
[35] F. Zhang, J. Zhao, T. Shan, H. Hidaka, E. Pelizzetti, N. Serpone, Appl. Catal. B: Environ. 15 (1998) 147–156.
[36] M. Muruganandham, M. Swaminathan, Sol. Energy Mater. Sol. Cells 81 (2004) 439–457.
[37] A.A. Khodja, T. Sehili, J.F. Pilichowski, P. Boule, J. Photochem. Photobiol. A: Chem. 141 (2001) 231–239.
[38] S.K. Pardeshi, A.B. Patil, J. Hazard. Mater. 163 (2009) 403–409.
[39] G. Chen, L. Lei, P.L. Yue, Ind. Eng. Chem. Res. 38 (1999) 1837–1843.